

Vitrification and crystallization of poly(butylene-2,6-naphthalate)

Koji Nishida^{a,*}, Evgeny Zhuravlev^b, Bin Yang^b, Christoph Schick^b, Yasuhiro Shiraishi^a, and
Toshiji Kanaya^a

^a *Institute for Chemical Research, Kyoto University, Uji, Kyoto 611-0011, Japan*

^b *Institute of Physics, University of Rostock, Wismarsche Str. 43-45, 18051 Rostock, Germany*

* Corresponding author. Tel.: +81-774-38-3141; fax: +81-774-38-3146.

E-mail address: knishida@scl.kyoto-u.ac.jp (K. Nishida).

Keywords:

Poly(butylene-2,6-naphthalate) (PBN)

Vitrification

Mesophase

Nucleation

Crystallization

ABSTRACT

The differential fast scanning calorimetry (DFSC) technique has been successfully applied to study the vitrification and crystallization of poly(butylene-2,6-naphthalate) (PBN). The cooling rate larger than 6,000 K/s could make the PBN vitrify and the cooling rate larger than 30,000 K/s reduced effectively the development of the active nuclei. The critical cooling rate of 30,000 K/s is three times as large as that of the recently reported poly(ϵ -caprolactone) (PCL)'s. Namely, it turned out that PBN is a hard-to-vitrify polymer. The heating rate faster than 7,000 K/s could prevent the cold crystallization from the proper glassy state. In the less severe cooling and heating rates than 30,000 K/s and 7,000 K/s, respectively, a variety of structure formations, such as the nucleation, the mesophase formation, the crystallization and their multiple melting behaviors, have been observed.

1. Introduction

In general, heterogeneity, whether or not it is intentionally added, assists effectively the nucleation process in solidification, especially at the small supercooling state [1,2]. It has been considered that also polymer crystallizations in many cases are initiated by the mechanism of heterogeneous nucleation. With increasing the degree of supercooling, the driving force for the nucleation increases. Accordingly, the chance of homogeneous nucleation increases relatively [2,3].

In some polymers, the temperature dependence of the nucleation and/or crystallization rates show a bimodal distribution [4-7]. Poly(ϵ -caprolactone) (PCL) is a typical example that shows such a bimodal behavior in the nucleation mechanism [8,9]. It is obvious that the heterogeneous and homogeneous nucleation mechanisms are dominant in the higher and lower temperature regions, respectively. External nucleating additives to PCL, e.g. carbon nanotubes, further assisted the nucleation in the higher temperature region of the bimodal distribution, whereas they did not affect nucleation in the lower temperature region [9]. Namely, the nucleation mechanism in the lower temperature region is considered a spontaneous process [10,11] occurring even in the homogeneous matrix.

Isotactic polypropylene (iPP) also shows such a bimodal behavior on cooling from the melt [5,10,12-14]. By the same token, the heterogeneous and homogeneous nucleation mechanisms are dominant in the higher and lower temperature regions, respectively. A

difference in the case of iPP from the former case is that the structure is frozen in the form of mesophase [15-22] as a result of the homogeneous nucleation.

Poly(butylene-2,6-naphthalate) (PBN) has a common property with iPP in terms of the mesophase formation [23]. However, the process of structure formation of PBN on cooling from the melt is much more complicated than the case of iPP. In the temperature region of small supercooling ($> ca. 160\text{ }^{\circ}\text{C}$), the crystallization occurred directly from the melt initiated by the heterogeneous nucleation. In an intermediate temperature range ($ca. 130 - 160\text{ }^{\circ}\text{C}$) the mesophase formed transiently and the crystallization proceeded successively via the mesophase [7]. Furthermore, such a mesophase-mediated crystallization of PBN proceeded much faster than the direct crystallization from the melt. Probably this particular property makes it difficult to obtain the glassy state of PBN and to understand the behavior of PBN in the large supercooling state.

In kinetic and also technical aspects, the mesophase of iPP is obtained by the cooling from the melt at a rate faster than $ca. 100\text{ K/s}$, preventing the crystallization which is initiated by the heterogeneous nucleation [5, 24-25]. Furthermore, cooling at a rate faster than $1,000\text{ K/s}$ also prevents the mesophase formation in iPP, which is initiated by the homogeneous nucleation, and consequently the glassy amorphous iPP is obtained [24,26]. For PCL the cooling rate $1,000\text{ K/s}$ prevents the crystallization from the melt and $10,000\text{ K/s}$ suppresses the formation of any nuclei that will be activated in the subsequent heating process [8,27]. However, in PBN the mesophase formation could not be prevented by cooling faster than

1,000 K/s [7]. Thus, the exploration of the vitrification and the structure formation of PBN in the large supercooling state is a challenging subject.

Recent development of the differential fast scanning calorimetry (DFSC) technique [28,29] has achieved a breakthrough on the issue. In this study by employing the DFSC, we have determined a critical cooling rate that makes PBN vitrify without developing any structures during cooling and also determined a critical heating rate that also prevents the structure formation during heating from the glassy state. In other words, a smaller heating rate than such a critical heating rate will reveal a variety of structure formations of PBN, such as the cold mesophase formation, the cold crystallization and their melting.

2. Experimental

The material for the present study is PBN pellets having an intrinsic viscosity of 1.40 dL/g, which are the same materials used in the previous study [23]. The structures of amorphous, mesophase and crystal observed by wide angle X-ray diffraction (WAXD) for the same PBN can be seen in [23] for reference.

The differential fast scanning calorimetry (DFSC) has been conducted using a sensor XI-296 (Xensor Integration, NL). The sample had a dimension of ca. 30 μm in diameter and ca. 10 μm in thickness. Taking the density of PBN (= ca. 1.3 g/cm^3) into consideration, the mass of the sample was estimated to be in the order of several nanograms. The details of the DFSC

measurements and the standard procedure of data analysis are described elsewhere [28,29]. In order to achieve the purpose mentioned in the introduction, the time-temperature scheme illustrated in Fig. 1 was employed. The history of sample was erased for 10 ms at 600 K, which is sufficiently higher than the equilibrium melting temperature of PBN ($T_m^0 = \text{ca. } 550 \text{ K}$) [30]. Then the samples were quenched at various cooling rates (R_C) between 2 and 60,000 K/s down to 95 K. We refer to this process as “previous cooling”. The destined temperature 95K of the previous cooling is sufficiently lower than the glass transition temperature of PBN ($T_g = \text{ca. } 315 \text{ K}$) [23,31]. All of the data in this study were collected during heating scans, which were conducted at various heating rates (R_H) between 1,000 and 10,000 K/s preceded by the previous cooling processes. The measured events in these heating scans should reflect the various transitions, such as vitrification, nucleation, crystallization and so on, which have happened in the previous cooling process.

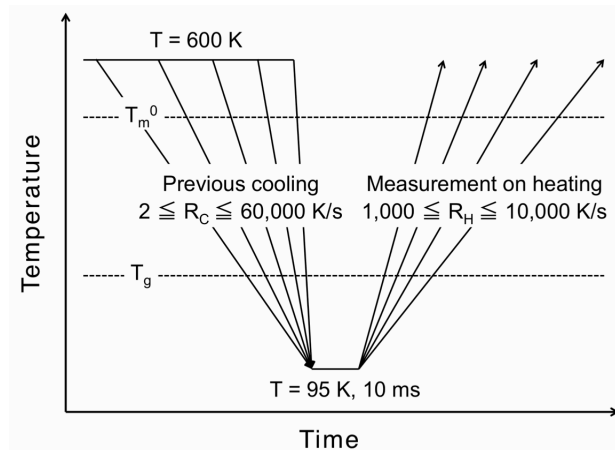


Fig. 1. Time-temperature scheme for the previous cooling process and the DFSC measurements on heating.

3. Results and discussion

3.1. Vitrification and structure formation

Fig. 2 shows a DFSC curve measured at a heating rate $R_H = 10,000$ K/s preceded by the previous cooling at a cooling rate $R_C = 60,000$ K/s. These cooling and heating rates are on the safe side in order to vitrify on cooling and devitrify on heating without any structure formations. The detail of the minimal requirement for the vitrification and devitrification without structure formations will be discussed later. Only a heat capacity step due to the glass transition was observed. Thus the DFSC technique has been proven to be applicable to the vitrification of PBN, namely the primary purpose of the present work has been achieved. On the present condition of the measurement, the onset temperature of the heat capacity increase appears at around 315 K and the midpoint of the heat capacity step is found at around 365 K, respectively. Those values relating to the glass transition are susceptible to the condition of the experiment, since the glass transition is essentially a non-equilibrium dynamic process. However, incidentally the onset temperature corresponds approximately to the previously reported one that was determined by a temperature-modulated DSC (TMDSC) method [23].

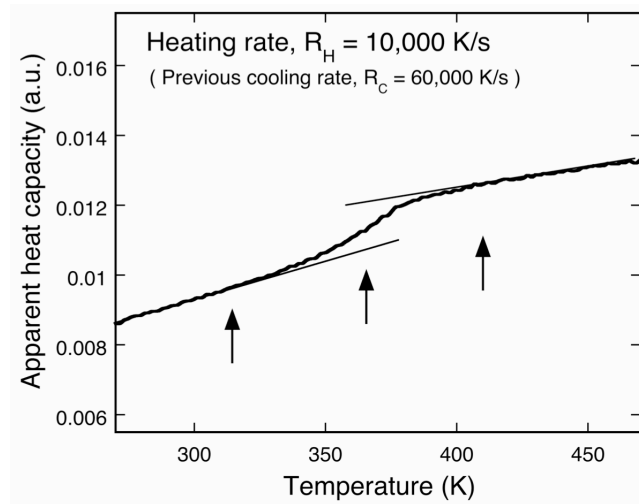


Fig. 2. DFSC curve measured at a heating rate $R_H = 10,000$ K/s preceded by the previous cooling at a cooling rate $R_C = 60,000$ K/s.

Fig. 3 shows a full set of the DFSC curves measured at a heating rate $R_H = 2,000$ K/s preceded by the previous cooling at various cooling rates R_C covering from 2 to 60,000 K/s. In contrast to the simple heat capacity step as was shown in Fig. 2, a variety of effects, such as a heat capacity step, an exothermic peak and multiple endothermic peaks, were observed.

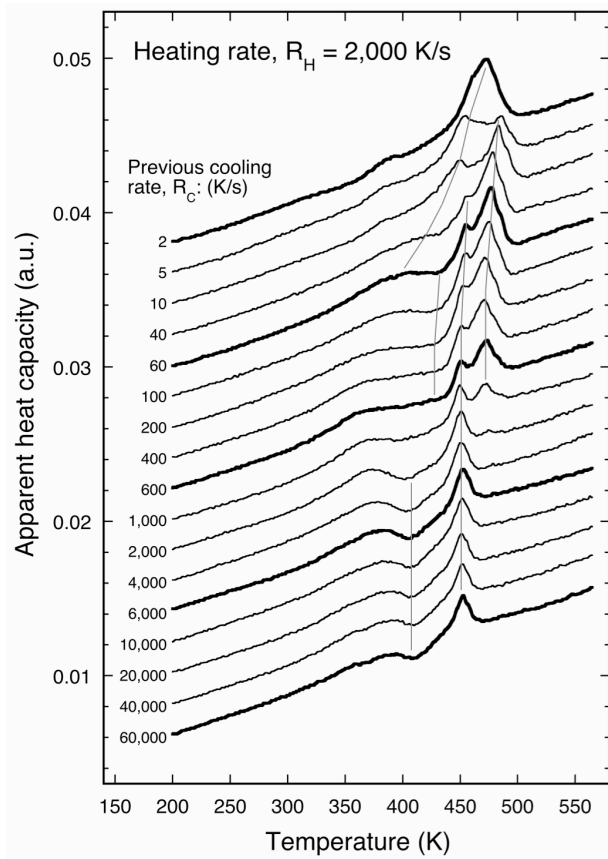


Fig. 3. DSC curves measured at a heating rate $R_H = 2,000$ K/s preceded by the previous cooling at various cooling rates R_C covering from 2 to 60,000 K/s.

These behaviors, except for the glass transition, can be divided broadly into five categories as is illustrated in Fig. 4. As was clarified by Cavallo, et al., the mesophase formed first and the crystallization proceeded subsequently when PBN was cooled from the molten state [7]. Taking these facts into consideration, the following interpretations for the five categories should be reasonable. The exothermic peak (I) that appears in the lowest

temperature region on heating is assumed the mesophase formation from devitrified amorphous. This peak was observed only when the previous cooling rate is large enough ($R_C > 2,000$ K/s). When the previous cooling rate is large enough, the heterogeneous nucleation is effectively prevented and the sample vitrifies, accordingly the exothermic process appearing first on heating is considered the mesophase formation that is assisted by the homogeneous nucleation mechanism in the state of large supercooling. The mesophase, which formed in the heating process, melts in the endothermic peak (II). The enthalpy of the exothermic peak (I) and that of the endothermic peak (II) essentially compensates each other, because any ordered structures, which may produce the net enthalpy of melting, did not form when the previous cooling rate R_C was large enough as was proven in Fig. 2. With decreasing the previous cooling rate ($R_C < 2,000$ K/s), the amount of the mesophase and/or the number of active nuclei, which have formed in the previous cooling process, should increase. These mesophase and/or active nuclei should assist the cold crystallization. Therefore, the exothermic peak (III) that appears in the higher temperature region than the peak (I) is considered the cold crystallization on heating. The crystal, which formed in the heating process, melts in the endothermic peak (IV). With decreasing the previous cooling rate, the amount of the ordered structures, which formed in the previous cooling process, increases. Finally, when the previous cooling rate is small enough, most of the structure formations have already finished in the previous cooling process. Accordingly, the chance for the reorganization, which produces the exothermic enthalpy, becomes very small. Therefore, endothermic peak (V) that appears when the

previous cooling rate is small enough is attributable to mainly the melting of the original crystal that formed already in the previous cooling process. In addition to these major contributions (I) - (V), other contributions may exist, e.g. a shoulder at ca. 490 K in the DFSC curve observed for the previous cooling $R_C = 60$ K/s. It maybe concerns the multiple melting behavior of PBN crystallized at higher temperature or at smaller cooling rate [30,32], unfortunately, the signal is too weak and overlap with another peak to identify the origin of those minor contributions at this moment.

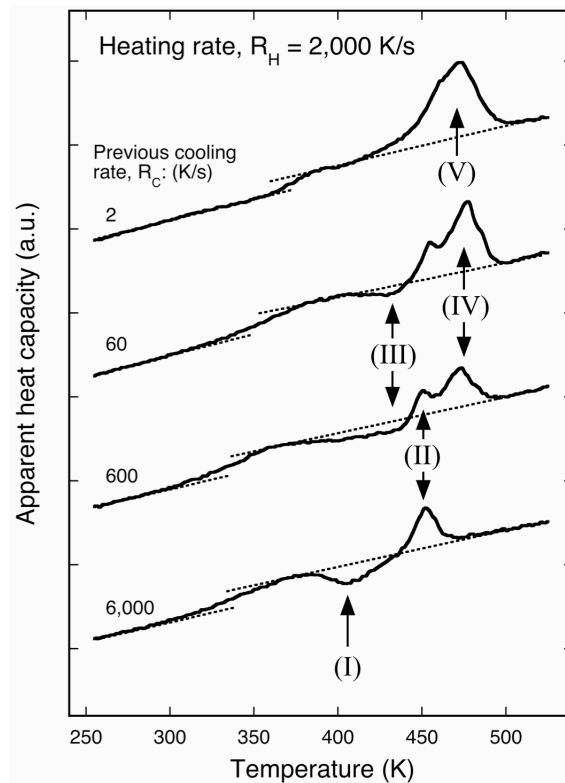


Fig. 4. Representative of DFSC curves illustrating five categories of exo- and endothermic peaks (I) - (V).

In order to reinforce the above-mentioned identifications, the trajectories of the temperatures of the peaks (I) - (V) are summarized in Fig. 5. When the well-resolved peaks were observed in Fig. 3 the point of data was plotted with marker in Fig. 5. However, when the peaks were not resolved well or very broad, the trends were just connected or extended with the dotted lines without the marker. The devitrified amorphous transforms into the mesophase (I) at around 410 K and the mesophase melts (II) at around 450 K. These temperatures are nearly independent of the previous cooling rate. The processes (I) and (II) form a pair excepting that the previous cooling rate R_C is less than 2,000 K/s. Small portion of the mesophase forms in the previous cooling process, i.e. the original mesophase, when $R_C < 2,000$ K/s. This original mesophase should contribute to the melting peak (II). The melting temperatures of the original mesophase and the mesophase that forms in the heating process are indistinguishable; this is probably because the original mesophase forms incidentally also at around 410 K [7]. The cold crystallization occurs (III) at around 430 K and the crystal, which formed in the heating process, melts (IV) at around 475 K. By the same token, the processes (III) and (IV) form a pair excepting that the previous cooling rate R_C is less than 40 K/s. When $R_C < 40$ K/s, the temperature region of the cold crystallization (III) is likely to intersect with that of the melting of the original crystal (V). Therefore, the peak separation becomes difficult in this region of the previous cooling rate. Of all transitions, the melting temperature of the original crystal (V) is strongly affected by the previous cooling rate. Both the melting temperature and the amount of the original crystal decrease drastically with

increasing the previous cooling rate. To the contrary, the melting temperature and the amount of the original crystal increase and should get close to certain constant values at the smallest limit of the previous cooling rate, however, unfortunately the extent of the previous cooling rate in the present study is not sufficient to show those behavior clearly.

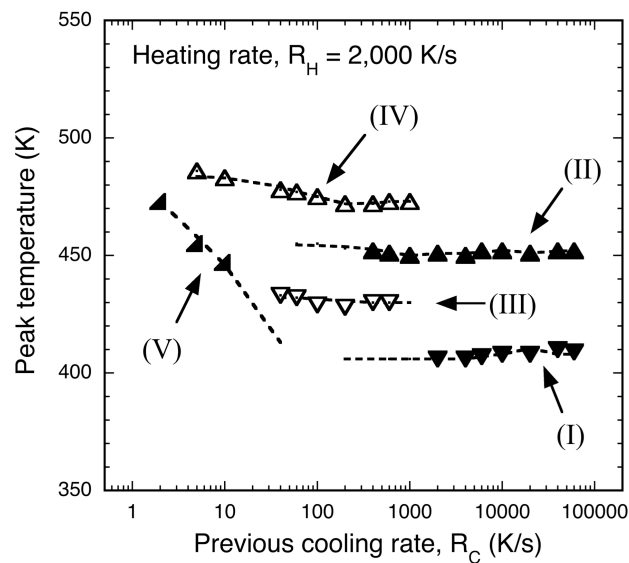


Fig. 5. Trajectories of five categories of exo- and endothermic peaks (I) - (V).

3.2. Critical cooling and heating rates that prevent structure formation

Fig. 6 shows the net enthalpy (upper panel) and the exothermic enthalpy (lower panel) as a function of the previous cooling rate for the case of a heating rate $R_H = 2,000$ K/s. Here we refer to the difference between the endothermic enthalpy (positive part) and the exothermic enthalpy (negative part) in Fig. 4 as the net enthalpy. The base lines used for the

evaluation of the enthalpies are shown by the dotted lines in Fig. 4. The net enthalpy is a measure of the amount of the already formed ordered structure at the end of the previous cooling process. That includes the crystal and the mesophase. The net enthalpy decreases monotonously with increasing the previous cooling rate and becomes zero when the previous cooling rate $R_C \geq 6,000$ K/s (rather on the safe side). Regarding the net enthalpy, similar trends are observed at other heating rates; they are found within the vertical bar drawn in Fig. 6. The length of the bar becomes less than the size of the plotted symbols when $R_C \geq 4,000$ K/s. It can safely be said that any ordered structures, which may produce the net enthalpy of melting, did not form when $R_C \geq 6,000$ K/s, regardless of the heating rate. The previous cooling rate $R_C = 6,000$ K/s corresponds to the minimal requirement for the vitrification of PBN.

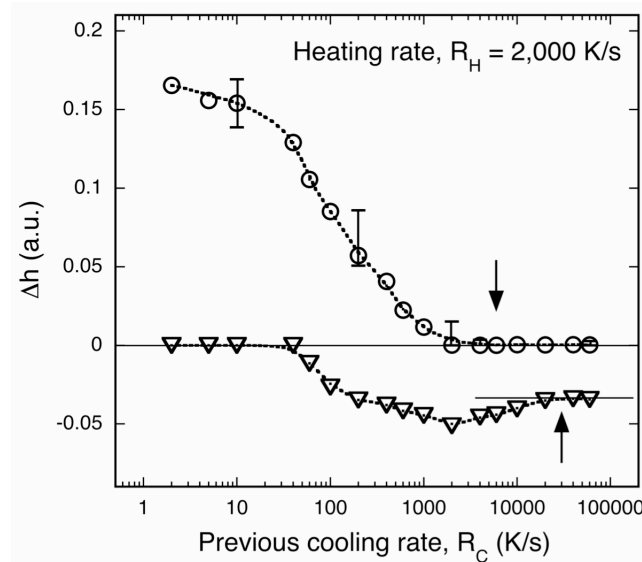


Fig. 6. Net enthalpy (upper panel) and exothermic enthalpy (lower panel) as a function of the previous cooling rate for the case of a heating rate $R_H = 2,000$ K/s.

On the other hand, the exothermic enthalpy (lower panel in Fig. 6) is a measure of the density of active nuclei that assist the formation of the ordered structures in the heating process [8]. The dependence of the exothermic enthalpy on the previous cooling rate is not monotonous. When the previous cooling rate is slow enough, most of the crystallization already finished in the previous cooling process. Namely, additional structure formations, which produce exothermic enthalpy, hardly occur in the subsequent heating process. With increasing the previous cooling rate, the amount of the already formed crystal decreases (see, upper panel), in other words, the room for the cold crystallization increases. However, the previous cooling rate has an antagonistic effect to the exothermic enthalpy. Too much previous cooling rate suppresses the chance to form the active nuclei that assists the cold crystallization and the mesophase formation. That is why the exothermic enthalpy shows a maximum in an intermediate region of the cooling rate.

The exothermic enthalpy still shows the dependence on the previous cooling rate even when $R_c \geq 6,000$ K/s, although the net enthalpy already became zero in the corresponding region. The dependence of the exothermic enthalpy on the previous cooling rate implies that the apparently vitrified PBN contains different degree of the nucleation ability. Finally, the exothermic enthalpy levels off when $R_c \geq 30,000$ K/s. The cooling rate $R_c = 30,000$ K/s corresponds to the critical cooling rate where PBN fully vitrifies without the development of the active nuclei. This value is about five times as large as that of the minimal requirement of the cooling rate.

The exothermic enthalpy depends strongly on the heating rate in addition to the previous cooling rate, whereas the net enthalpy showed little difference regarding the heating rate. Fig. 7 shows the exothermic enthalpy as a function of the previous cooling rate for the different rates of heating. The lower is the heating rate, the more the exothermic enthalpy is enhanced, and *vice versa*.

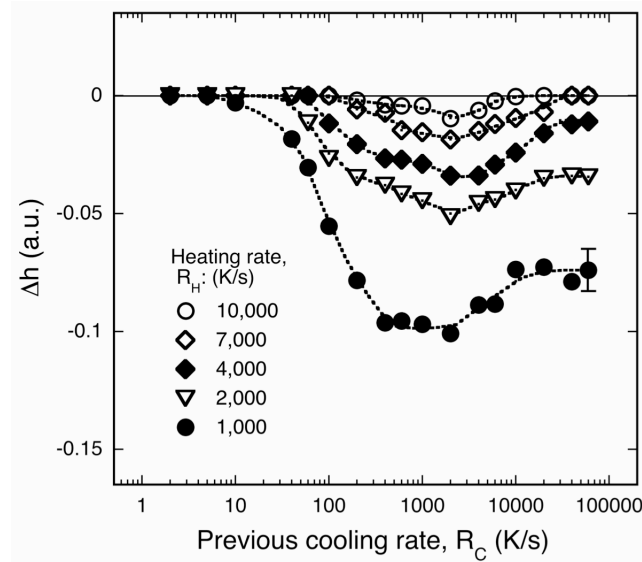


Fig. 7. Exothermic enthalpy as a function of the previous cooling rate for the different rates of heating.

Fig. 8 shows the exothermic enthalpy as a function of the heating rate for the fully vitrified PBN ($R_C = 60,000$ K/s). The exothermic enthalpy becomes zero when $R_H \geq 7,000$ K/s.

The heating rate $R_C = 7,000$ K/s corresponds to the minimal requirement of the heating rate where fully vitrified PBN devitrifies without the development of the active nuclei.

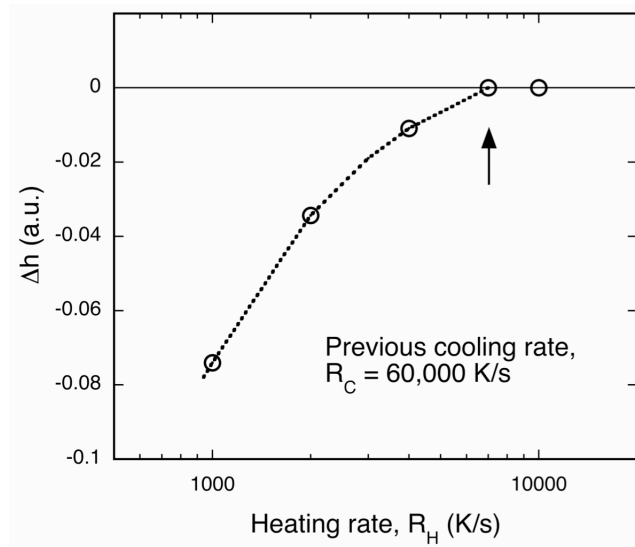


Fig. 8. Exothermic enthalpy as a function of the heating rate for the fully vitrified PBN ($R_C = 60,000$ K/s).

In comparison with other crystalline polymers, the critical cooling rate 30,000 K/s is considerably large. PCL is a typical fast crystallizing polymer [8,27], but the critical cooling rate for full vitrification of the additive-free PCL is 10,000 K/s [8] as was mentioned in the introduction. Namely, the critical cooling rate of PBN is three times as large as that of PCL. At this moment, we have not heard about the critical cooling rate of polyethylene (PE) yet, but it has been turned out that PBN is one of the extremely hard-to-vitrify polymers. The major

reason is considered that the homogenous nucleation mechanism works actively in the large supercooling state, as is the case in iPP and PCL. The homogenous nucleation mechanism could be still active below the nominal T_g . The densification below the nominal T_g may also assist the nucleation, as is the case in PCL [9]. Those speculations should be clarified in the future work.

4. Conclusions

The differential fast scanning calorimetry (DFSC) technique has been applied to study the vitrification and crystallization of poly(butylene-2,6-naphthalate) (PBN). Although PBN is one of the very fast crystallizing polymers and was hard to get its proper glassy state, it has turned out that the cooling rate larger than 6,000 K/s makes the PBN vitrify. Furthermore, the cooling rate larger than 30,000 K/s reduced effectively the development of the active nuclei. This critical value is three times as large as that of poly(ϵ -caprolactone) (PCL) which is a typical fast crystallizing polymer. In addition, the heating rate faster than 7,000 K/s could prevent the cold crystallization from the proper glassy state. A variety of transitions, such as the mesophase formation, the crystallization and their multiple melting behaviors, have been observed on the less severe cooling and heating conditions than the above-mentioned boundary condition. Thanks to the trajectory analysis of the exo- and endothermic peaks

covering the wide range of previous cooling rates, the reliable identification of the complicated transition behavior has become possible, which was never possible with a single heating scan. Lastly, the isothermal low temperature annealing experiments in the vicinity of the glass transition temperature will prospect the further understanding of the hard-to-vitrify behavior of PBN.

Acknowledgements

This research was supported by FY 2013 Researcher Exchange Program between Japan Society for the Promotion of Science (JSPS) and Deutscher Akademischer Austausch Dienst (DAAD) awarded to K. N.

References

- [1] D. Turnbull, Kinetics of heterogeneous nucleation, *J. Chem. Phys.* 18 (1950) 198-203.
- [2] D. Turnbull, Kinetics of solidification of supercooled liquid mercury droplets, *J. Chem. Phys.* 20 (1952) 411-424.
- [3] R.L. Cormia, F.P. Price, D. Turnbull, Kinetics of crystal nucleation in polyethylene, *J.*

Chem. Phys. 37 (1962) 1333-1340.

[4] D. Heberer, A. Keller, V. Percec, Interrelation between crystallization and liquid crystal formation: a calorimetric and polarizing microscopical study on a monotropic polymer system, *J. Polym. Sci.: Part B Polym. Phys.*, 33 (1995) 1877-1894.

[5] C. Silvestre, S. Cimmino, D. Duraccio, C. Schick, Isothermal crystallization of isotactic poly(propylene) studied by superfast calorimetry, *Macromol. Rapid Commun.* 28 (2007) 875–881.

[6] B. Heck, E. Perez, G. Strobl, Two competing crystallization modes in a smectogenic polyester, *Macromolecules* 43 (2010) 4172–4183.

[7] D. Cavallo, D. Mileva, G. Portale, L. Zhang, L. Balzano, G.C. Alfonso, R. Androsch, Mesophase-mediated crystallization of poly(butylene-2,6-naphthalate): an example of Ostwald's rule of stages, *ACS Macro Lett.* 1 (2012) 1051-1055.

[8] E. Zhuravlev, J.W.P. Schmelzer, B. Wunderlich, C. Schick, Kinetics of nucleation and crystallization in poly(ϵ -caprolactone) (PCL), *Polymer* 52 (2011) 1983-1997.

[9] E. Zhuravlev, A. Wurm, P. Pötschke, R. Androsch, J.W.P. Schmelzer, B. Wunderlich, C. Schick, Kinetics of nucleation and crystallization of poly(ϵ -caprolactone) – multiwalled carbon nanotube composites, *Eur. Polym. J.* 52 (2014) 1–11.

[10] F.L. Binsbergen, Heterogeneous nucleation in the crystallization of polyolefins. III. Theory and mechanism, *J. Polym. Sci.: Polym. Phys. Ed.*, 11 (1973) 117-135.

[11] A. Mamun, S. Umemoto, N. Ishihara, N. Okui, Influence of thermal history on primary

nucleation and crystal growth rates of isotactic polystyrene, *Polymer* 47 (2006) 5531–5537.

[12] A. Ghijssels, N. Groesbeek, C.W. Yip, Multiple crystallization behaviour of polypropylene/thermoplastic rubber blends and its use in assessing blend morphology, *Polymer* 23 (1982) 1913–1916.

[13] M. Arnal, A.J. Müller, P. Maiti, M. Hikosaka, Nucleation and crystallization of isotactic poly(propylene) droplets in an immiscible polystyrene matrix, *Macromol. Chem. Phys.* 201 (2000) 2493–2504.

[14] D. Cavallo, F. Azzurri, R. Floris, G.C. Alfonso, L. Balzano, G.W. Peters, Continuous cooling curves diagrams of propene/ethylene random copolymers. The role of ethylene counits in mesophase development, *Macromolecules* 43 (2010) 2890–2896.

[15] G. Natta, Progress in five years of research in stereospecific polymerization, *SPE. J.* 15 (1959) 373–382.

[16] R.L. Miller, On the existence of near-range order in isotactic polypropylenes, *Polymer* 1 (1960) 135–143.

[17] C.C. Hsu, P.H. Geil, H. Miyaji, K. Asai, Structure and properties of polypropylene crystallized from the glassy state, *J. Polym. Sci., Part B: Polym. Phys.* 24 (1986) 2379–2401.

[18] S. Piccarolo, M. Saiu, V. Brucato, G. Titomanlio, Crystallization of polymer melts under fast cooling. II. High-purity iPP, *J. Appl. Polym. Sci.* 46 (1992) 625–634.

[19] I. Coccorullo, R. Pantani, G. Titomanlio, Crystallization kinetics and solidified structure in iPP under high cooling rates, *Polymer* 44 (2003) 307–318.

- [20] T. Konishi, K. Nishida, T. Kanaya, K. Kaji, Effect of isotacticity on formation of mesomorphic phase of isotactic polypropylene, *Macromolecules* 38 (2005) 8749–8754.
- [21] R. Androsch, M.L.D. Lorenzo, C. Schick, B. Wunderlich, Mesophases in polyethylene, polypropylene, and poly(1-butene), *Polymer* 51 (2010) 4639-4662.
- [22] K. Nishida, K. Okada, H. Asakawa, G. Matsuba, K. Ito, T. Kanaya, K. Kaji, In situ observations of the mesophase formation of isotactic polypropylene—A fast time-resolved X-ray diffraction study, *Polym. J.* 44 (2012) 95-101.
- [23] T. Konishi, K. Nishida, G. Matsuba, T. Kanaya, Mesomorphic phase of poly(butylene-2,6-naphthalate), *Macromolecules* 41 (2008) 3157-3161.
- [24] F. De Santis, S. Adamovsky, G. Titomanlio, C. Schick, Scanning nanocalorimetry at high cooling rate of isotactic polypropylene, *Macromolecules* 39 (2006) 2562–2567.
- [25] Q. Zia, R. Androsch, H.-J. Radusch, S. Piccarolo, Morphology, reorganization, and stability of mesomorphic nanocrystals in isotactic polypropylene, *Polymer* 47 (2006) 8163–8172.
- [26] F. De Santis, S. Adamovsky, G. Titomanlio, C. Schick, Isothermal nanocalorimetry of isotactic polypropylene, *Macromolecules* 40 (2007) 9026–9031.
- [27] A. Wurm, E. Zhuravlev, K. Eckstein, D. Jehnichen, D. Pospieck, R. Androsch, B. Wunderlich, C. Schick, Crystallization and homogeneous nucleation kinetics of poly(ϵ -caprolactone) (PCL) with different molar masses, *Macromolecules* 45 (2012) 3816-3828.

- [28] E. Zhuravlev, C. Schick, Fast scanning power compensated differential scanning nano-calorimeter: 1. The device, *Thermochim. Acta* 505 (2010) 1-13.
- [29] E. Zhuravlev, C. Schick, Fast scanning power compensated differential scanning nano-calorimeter: 2. Heat capacity analysis, *Thermochim. Acta* 505 (2010) 14-21.
- [30] M.Y. Ju, F.C. Chang, Multiple melting behavior of poly(butylene-2,6-naphthalate), *Polymer* 42 (2001) 5037-5045.
- [31] T.Yamanobe, H. Matsuda, K. Imai, A. Hirata, S. Mori, T. Komoto, Structure and physical properties of naphthalene containing polyesters I. Structure of poly(butylene 2,6-naphthalate) poly(ethylene 2,6-naphthalate) as studied by solid state NMR spectroscopy, *Polym. J.* 28 (1996) 177-181.
- [32] M. Yasuniwa, S. Tsubakihara, T. Fujioka, Y. Dan, X-ray studies of multiple melting behavior of poly(butylene-2,6-naphthalate), *Polymer* 43 (2005) 8306-8312.